Spectral Characteristics of the Various Prototropic Species of 2-(4′-*N*,*N*-Dimethylaminophenyl)pyrido[3,4-*d*]imidazole

G. Krishnamoorthy and S. K. Dogra*

Department of Chemistry, Indian Institute of Technology Kanpur, Kanpur-208016, India

Received November 20, 1998

Spectral characteristics of 2-(4′-*N*,*N*-dimethylaminophenyl)pyrido[3,4-*d*]imidazole (DMAPPI) have been studied in two different solvents and H_0/pH/H_- range of −10 to +16. Combining the results observed in the absorption, fluorescence, and fluorescence excitation spectra, it is found that (i) only one kind of monoanion (deprotonation of >N−H group) and one kind of trication, (ii) two kinds of monocations (MC1 and MC3) in the ground state and (MC2 and MC3) in the excited singlet state, and (iii) three kinds of dications (DC1, DC2, and DC3) are observed. Semiempirical quantum mechanical calculations (AM1) have been carried out on all kinds of ionic species and their resonating structures. The spectral characteristics have been assigned to various prototropic species combining the experimental and theoretical results.

1. Introduction

Chemistry of heterocycles is always a subject of interest. Besides the fundamental interest in the area of heterocycles, these compounds can be used as intermediates,[1] and fine products for drugs,[2,3] color industries,[4] laser dyes,[5] complex-forming agents,[6,7] redox systems for solar energy,[8] and organized assemblies.[9] Besides these applications, another area of interest is the study of hydrogen transfer and the prototropism with suitable substituents, for example, amino-, hydroxy-,[10−15] and aminophenylbenzazoles.[16] It has been observed that usually these prototropic equilibria are different in the excited singlet (S_1) state than the ground (S_0) state and may involve intramolecular proton transfer.[17,18]

During our recent studies[19−24] on the prototropic reactions of 2-(4′-aminophenyl, AP) 2-(4′-*N*,*N*-dimethylamino-phenyl, DMAP) benzazoles (benzimidazole, BI; benzoxazole, BO; benzothiazole, BT, Scheme 1), it has been shown that two kinds of monocations (MCs) are formed, both in the S_0 and S_1 state, i.e., MC1 is obtained by protonating the $-NH_2$ or $-NMe_2$ group, whereas MC2 is formed by protonating the =N− atom of the imidazole ring. The relative populations of MC1 and MC2 depend on the electronegativity of the benzazole ring and the polarity of the solvents. For example, in the aqueous medium MC1 (large polar) is more predominant, whereas MC2 (less polar) is present largely in nonpolar medium. Further, the major component in the APBI or DMAPBI is MC2 and its proportion decreases if BI is replaced by BT and BO in the given order. Fasani et al.[25] in their study on the prototropic reactions on 2-(4′-aminophenyl)-pyrido-, -oxa-, -thia-, and imidazoles have shown that only one kind of MC (MC1) is formed in all the molecules, which seems to be highly improbable. So we have synthesized DMAPPI (Scheme 2) and carried out the studies from two angles: (i) to find out the site of first protonation as well as to see whether there is only one kind of MC or different kind of MCs and (ii) to see whether any red-shifted emission attributed to a twisted intramolecular charge transfer (TICT) is observed from the prototropic species or not.

Scheme 1

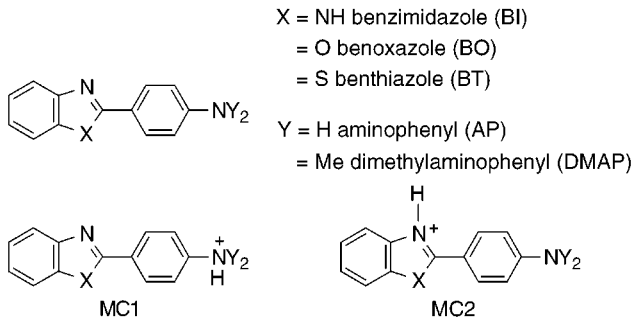

(1) Barni, E.; Savarino, P.; Viscardi, G. *Trends Heterocycl. Chem.* **1991**, *2*, 27.
(2) Clark, R. L.; Pessonlando, A. A.; Witzel, B. E.; Lanza, T. J.; Shen, T. *J. Med. Chem.* **1978**, *21*, 1158.
(3) Middelton, R. W.; Wibberly, D. J. *J. Heterocyl. Chem.* **1980**, *17*, 1757.
(4) James, T. H. *The Theory of the Photographic Process*, 4th ed.; MacMillan: New York, 1977.
(5) Barkova, L. A.; Gruzinskii, V. V.; Danilova, V. I.; Degtyarenko, K. M.; Kopylanova, T. N.; Kuznetsov, A. L. *Electron (Moscow)* **1981**, *8*, 1728.
(6) Massacesi, M.; Biddau, M.; Barni, E.; Savarino, P. *Inorg. Chim. Acta* **1984**, *82*, 27.
(7) Massacesi, M.; Pinna, R.; Mecera, G.; Strinna Erre, L.; Savarino, P. *Trans. Met. Chem.* **1988**, *13*, 116.
(8) Summers, L. A. *J. Heterocycl. Chem.* **1991**, *28*, 827.
(9) Gordon, P. F. In *The Chemistry and Application of Dyes*; Waring, D. R., Hallas, G., Eds.; Plenum Press: New York, 1990; Chapter 8.
(10) Swaminathan, M.; Dogra, S. K. *J. Am. Chem. Soc.* **1983**, *105*, 6223.
(11) Mishra, A. K.; Dogra, S. K. *Indian J. Chem.* **1985**, *24A*, 285.
(12) Phaniraj, P.; Mishra, A. K.; Dogra, S. K. *Indian J. Chem.* **1985**, *24A*, 913.
(13) Mishra, A. K.; Dogra, S. K. *J. Photochem.* **1985**, *29*, 435.
(14) Tway, P. C.; Love, L. J. C. *J. Phys. Chem.* **1982**, *86*, 5223, 5227.
(15) Roussilha, J.; Paillous, N. *J. Chim. Phys.* **1983**, *80*, 595.
(16) Dogra, S. K. *Proc. Indian Acad. Scn.* **1992**, *104*, 635.
(17) Mishra, A. K.; Dogra, S. K. *J. Photochem.* **1985**, *31*, 333.
(18) Santra, S.; Dogra, S. K. *Chem. Phys.* **1998**, *226*, 285.
(19) Mishra, A. K.; Dogra, S. K. *Bull. Chem. Soc. Jpn.* **1985**, *58*, 3587.
(20) Dey, J. K.; Dogra, S. K. *Chem. Phys.* **1990**, *143*, 97.
(21) Dey, J. K.; Dogra, S. K. *Bull. Chem. Soc. Jpn.* **1991**, *64*, 3142.
(22) Dey, J. K.; Dogra, S. K. *J. Phys. Chem.* **1994**, *98*, 3638.
(23) Krishnamoorthy, G.; Dogra, S. K. *J. Photochem. Photobiol. A: Chem.* **1999**, *123*, 109.
(24) Krishnamoorthy, G.; Dogra, S. K. *Chem. Phys.* **1999**, *243*, 45.
(25) Fasani, E.; Albini, A.; Savarino, P.; Viscardi, G.; Barni, E. *J. Heterocyl. Chem.* **1993**, *30*, 1041.

10.1021/jo9822986 CCC: $18.00
Published on Web 08/10/1999

Scheme 2

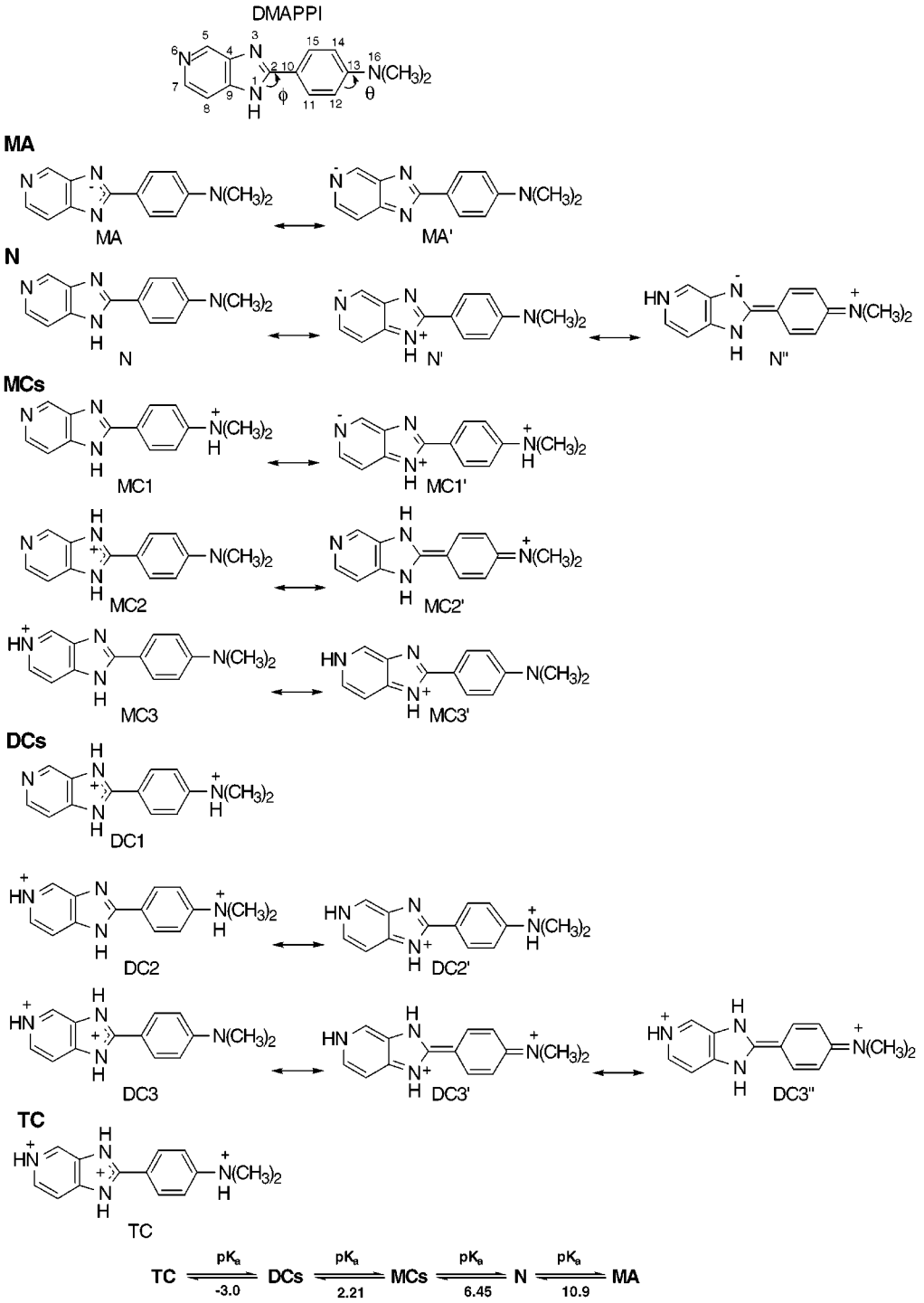

2. Materials and Methods

DMAPPI was prepared from 3,4-diaminopyridine and p-(*N*,*N*-dimethylamino)benzoic acid by the procedure reported in the literature.[26] The compound was purified by repeated crystallization from methanol. The purity of DMAPPI was checked by TLC and by verifying that the fluorescence excitation spectrum in cyclohexane was identical when the emission was monitored at different wavelengths. Cyclohexane (spectral grade, SD fine) was used as received. Methanol (E. Merck, Anal. R grade) was further purified by the method as described in the literature.[27] Both the solvents were checked for spurious fluorescence in the region of fluorescence measurements. Triply distilled water was used for pH solutions. Analytical grade H_2SO_4 (BDH), sodium hydroxide (Thomas Baker), and *o*-phosphoric acid (BDH) were used as received.

Aqueous solutions in the pH range 3−11 were prepared by mixing appropriate amounts of dilute ($\sim 10^{-3}$ M) solutions of NaOH and H_3PO_4. Hammett's acidity scale (H_0)[28] was used in preparing solutions of pH < 1.0. All the spectral measurements were carried out at the solute concentration of the order of 10^{-5} M. Fluorescence quantum yields were determined for

(26) Middleton, R. W.; Wibberely, D. G. *J. Heterocyl. Chem*. **1980**, *17*, 1757.

(27) Riddick, M. J.; Bunger, W. In *Organic Solvents*; Wiley-Interscience: New York, 1970; pp 632, 693.

(28) Jorgenson, M. J.; Hartter, D. R. *J. Am. Chem. Soc*. **1957**, *79*, 427.

Table 1. Different Parameters of the Various Prototropic Species of DMAPPI Obtained from the Semiempirical Quantum Mechanical Calculations (AM1)

	MA	N	MC1	MC2	MC3	DC1	DC2	DC3	TC
E_{iso} (eV)	−2798.633	−2810.762	−2817.643	−2818.556	−2818.356	−2822.574	−2823.099	−2822.928	−2824.430
E_{sol} (eV)			−2819.468	−2818.589	−2819.201	−2823.465	−2823.127	−2823.342	
ΔH_f (kCal)	76	111	267	246	251	469	456	460	741
a (Å)			5.23	5.28	5.27	5.26	5.24	5.23	
μ_g (D)	10.98	6.72	20.66	2.82	10.97	14.56	2.58	9.99	4.38
θ (deg)	−22.53	−16.75	−117.7	1.1	1.5	−117.4	117.3	−1.1	117.8
ϕ (deg)	−0.29	−31.6	−24.5	−2.9	6.8	49.4	33.8	1.8	−39.2
C_2-C_{10} (Å)	1.46	1.46	1.46	1.44	1.45	1.47	1.47	1.40	1.46
$C_{13}-N_{16}$ (Å)	1.43	1.40	1.47	1.37	1.38	1.47	1.45	1.35	1.47
TE[a] (nm)			306 (310)		361 (368)	312 (294)	340 (330)	411 (409)	

[a] TE = transition energy, obtained from ZINDO/S calculations. The figures in parentheses are the experimental values.

solutions having absorbances less than 0.1 at the excitation wavelength (λ_{exc}) and referred to quinine sulfate in 1 N H_2SO_4 ($\phi_{fl} = 0.55$).[29] For fluorimetric titrations, the solutions were excited at the isosbestic wavelength of the absorption spectra, i.e., 310 nm for the dication−monocation (DC−MC), 352 nm for the monocation−neutral (MC−N) and 333 nm for the neutral−monoanion (N−MA) equilibria. Absorption spectra were recorded on a Shimadzu UV190 spectrophotometer equipped with a 135U chart recorder. Steady-state fluorescence and fluorescence excitation spectra were recorded on a Fluorolog-3 (ISA Jobin Yvon-Spex Instruments S.A., Inc.) spectrofluorimeter, and all the spectra reported are corrected. The pH of the solutions were measured on a Toshniwal digital pH meter (Model CL54).

3. Semiempirical Quantum Mechanical Calculations

Scheme 2 shows that there can be three possible MCs (MC1, formed by protonating $-NMe_2$ group; MC2, formed by protonating the $=N_3-$ atom; and MC3, obtained by protonating the $=N_6-$ atom); three possible dications (DC1, protonation at the $-NMe_2$ group and the $=N_3-$ atom; DC2, protonation at the $-NMe_2$ group and the $=N_6-$ atom; and DC3, protonation at the $=N_3-$ and $=N_6-$ atoms); one trication (TC); and one monoanion (MA, obtained by deprotonation of >N−H moiety). The PC MODEL[30] program was used to obtain the starting geometry of each species. This program enabled us to draw the structure and optimize roughly the geometry of each species using the MM2 force field and generate the corresponding coordinates. The AM1 Program[31] (QCMP 137, MOPAC6/PC) was used to optimize the geometry of the species without using any constraints. The relevant parameters (the minimum energy, E_{iso}; dipole moment, μ_g; the dihedral angles θ between the dimethylamino group and the phenyl ring and ϕ between the aminophenyl ring and the pyridoimidazole (PI) ring; and bond distances C_2-C_{10} and $C_{13}-N_{16}$) are compiled in Table 1. Dipolar solvation energies (ΔE_s) in water were calculated using eq 1[32,33]

$$\Delta E_s = -(\mu_g^2/4\pi\epsilon_0 a^3)\,[(\epsilon - 1)/(2\epsilon + 1)] \qquad (1)$$

where μ_g is the dipole moment in the ground state, a is the Onsager cavity radius, and ϵ is the dielectric constant. In the present calculation, the cavity radius a for each species was obtained by taking 40% of the longest distance in the optimized geometry of the nonspherical species,[34] and the radii are compiled in Table 1. The energies (E_{sol}) thus obtained are also compiled in Table 1. AM1 calculations for the excited states taking configuration interactions into account were carried out in the MOPAC program. Since these are large molecular species these calculations have not been able to optimize the geometries in the S_1 state, and thus, no meaningful results were obtained. However, the transition energies for the MCs and DCs were obtained by performing ZINDO/S (an INDO method parametrized to reproduce UV−vis transitions) single-point calculations including the configuration interactions involving the five highest occupied and the five lowest unoccupied orbitals using HyperChem program.[35] The transition energies thus obtained are also compiled in Table 1.

4. Prototropic Species

DMAPPI possesses one acidic center (>NH) and three basic centers ($=N_3-$, $=N_6-$, and $-NMe_2$). As mentioned previously, there can be one MA at high pH, three possible MCs, three possible DCs, and one TC as shown in Scheme 2. Thus, the prototropic equilibrium for each combination will be considered separately.

4.1 Monoanion. The absorption spectra of the MA of DMAPPI (H_- 14.0) and its fluorescence spectra, when excited at 310, 330, and 350 nm are given in Figures 1 and 2b, respectively. Relevant data are compiled in Table 2. The absorption band maximum of the MA is blue shifted in comparison to the neutral (N) species, whereas dual fluorescence is observed when the solution containing the MA is excited at 310, 330, and 350 nm (Figure 2b). The shorter wavelength (SW) emission band (399 nm) is blue shifted and the longer wavelength (LW) emission (505 nm) is large red shifted in comparison to the normal emission, but the LW emission is nearly at the same wavelength as that of the TICT emission of the N species (Table 2). Both the emission band maxima and ϕ_{fl} of the MA are insensitive to the λ_{exc}. These results clearly suggest that both the emissions are occurring from the most relaxed excited states. Unlike neutral species,[36] the ϕ_{fl} of the LW emission of the MA is 2.5 times greater than that of the SW emission. The fluorescence excitation spectra recorded at 400, 420, 480, 500, and 520 nm are exactly similar to each other and to the absorption spectrum of the MA. Figure 2a depicts the fluorescence

(29) Meach, S. R.; Phillips, D. *J. Photochem.* **1983**, *23*, 193.
(30) Hinze, J.; Jaffe, H. H. *J. Am. Chem. Soc.* **1962**, *84*, 540.
(31) Dewar, M. J. S.; Zeobish, E. G.; Healy, E. F.; Stewart, J. J. P. *J. Am. Chem. Soc.* **1985**, *107*, 3092.
(32) Mataga, N.; Kubata, T. *Molecular Interactions and Electronic Spectra*; Marcel Dekker: New York, 1970.
(33) Letard, J. F.; Lapouyade, R.; Rettig, W. *Chem. Phys. Lett.* **1994**, *222*, 209.
(34) Lippert, E. *Z. Nauturforsch. A* **1955**, *10*, 541.
(35) Zener, M. Quantum Theory Project, University of Florida; HyperChem Release 5.0, Hypercube Inc., Waterloo, Canada.
(36) Krishnamoorthy, G.; Dogra, S. K. *Spectrochim. Acta A*, in press.

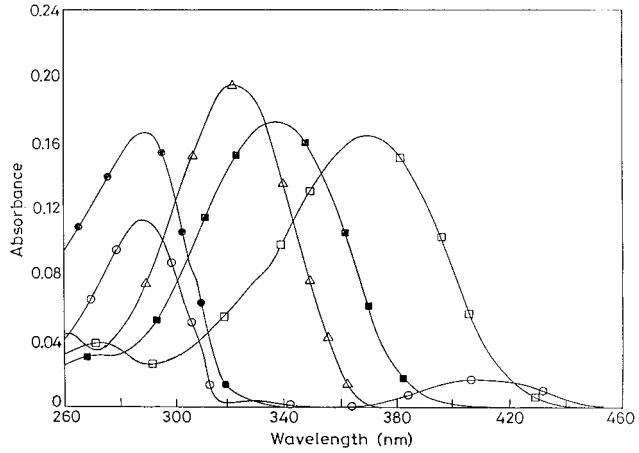

Figure 1. Absorption spectra of the various prototropic species of DMAPPI. −△−, MA (H_- 14.0); −■−, N (pH 9.0); −□−, MC (pH 4.0); −○− DC (pH 0.98); −●− TC (H_0 −10.4). [DMAPPI] = 0.5×10^{-5} M.

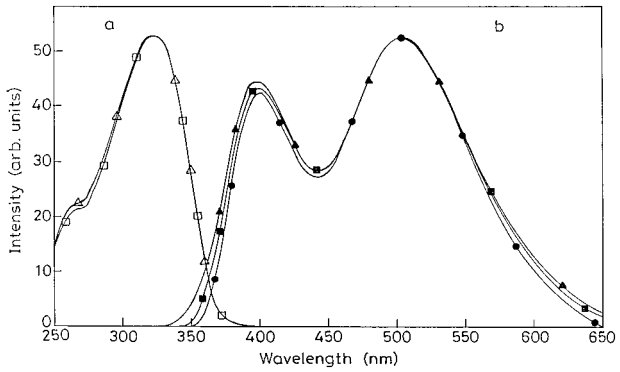

Figure 2. (a) Fluorescence excitation spectra of the MA of DMAPPI monitored at 400 −△− and 520 nm −□− at H_- 14; (b) Fluorescence spectra of the MA of DMAPPI. H_- 14.0, λ_{exc} = 310 nm −▲−; 330 nm −■−; 350 nm −●−. [DMAPPI] = 0.5×10^{-5} M (for comparison all spectra are given in same scale).

excitation spectra only at λ_{em} 400 and 520 nm. The pK_a value for the N−MA equilibrium has been determined using absorbance data and is found to be 10.9 (Table 3), which is much less than the similar deprotonation constant of 2-phenylbenzimidazole (2-PBI, 11.9).[37] The excited-state pK_a (pK_a*) value for the N−MA equilibrium was determined by the fluorimetric titration method (Figure 3), using λ_{exc} as λ_{isos} (333 nm). The value so obtained is similar to the ground-state pK_a value.

The absorption and the SW fluorescence spectra of the MA are blue shifted relative to those of the neutral species. This is contrary to what is normally observed for the deprotonation of the >NH group[38] and can be explained as follows. The resonance structures of DMAP-PI (N) can be written as either N′ or N″ (Scheme 2). The resonance structure N″ will lead to the increase in the charge density at N_3 and decrease in the bond lengths C_2-C_{10}, as well as in $C_{13}-N_{16}$. This will bring more planarity among the two rings and rigidity in the molecule, an increase in the pK_a value for the protonation of the $=N_3-$ atom, and red shifts in the spectral characteristics of DMAPPI. On the other hand, the resonance structure N′ will decrease the charge density at >NH and make it more acidic. The value of the deprotonation constant of the >NH group substantiates this. The dissociation of the >NH group leaves a negative charge on the PI ring. This negative charge is delocalized on both the pyrido and imidazole rings because of the resonating structures and may decrease the coplanarity of the PI and benzene rings. On the other hand, AM1 calculations carried out on the MA have shown that in comparison to neutral species the dihedral angle θ increases from −16.75° to −22.53°, whereas the dihedral angle ϕ decreases from −31.63° to −0.29°. In other words, the PI and benzene rings in the MA are more coplanar than those in the neutral species, whereas $-NMe_2$ becomes less coplanar in the MA. Thus, the blue shifts observed in the spectral characteristics of the MA when compared to the neutral species could be due to the reduced resonance effect of the lone pair of the terminal nitrogen atom of the $-NMe_2$ group. A similar behavior has also been observed in the deprotonation reaction of the >NH moiety of the 2-(4′-hydroxyphenyl)benzimidazole,[39] APBI,[19] and DMAPBI.[22]

The LW emission band of the MA can be assigned to the TICT state of the MA, because similar to the neutral DMAPPI,[36] the fluorescence excitation spectra recorded at 505 nm exactly resemble the absorption spectrum of the MA and are very large Stokes shifted (11060 cm^{-1}). A similar behavior has also been observed in DMAPBI and DMAPBT[22] and *p*-*N*,*N*-dimethylaminobenzoic acid (DMABA) at high pH,[40] where the electron-withdrawing group in each case is an anion. It is established[41] that in the organic solvents and for the same electron-donor group the TICT emission intensity increases with the increase in the electron-accepting property of the electron-withdrawing group. The increase (3.2 times that in the neutral) in the fluorescence quantum yield of the TICT band in the MA of the DMAPPI in aqueous medium suggests that the negative charge on the PI is more electron withdrawing than the neutral PI ring. Although the electron affinity data for the PI anion and PI neutral are not available, it is still difficult to understand the above behavior of PI anion. It may be thus pointed out that TICT emission in aqueous medium is different from that in organic solvents.

In the case of neutral DMAPPI,[36] the TICT emission is only observed in protic solvents, suggesting that the hydrogen bonding plays the major role in the TICT emission. It has been shown previously[36] that the hydrogen bonding of the solvent with PI ring leads the PI ring to be more planar with the benzene ring rather than twisting it, thereby facilitating the charge flow from DMAP group to PI ring. Thus, it was suggested that it is the twisting of the $-NMe_2$ group and the planarity of the PI ring with the benzene ring that leads to the TICT emission in polar solvents. It is also clear from AM1 calculations (Table 1) carried out on the MA of DMAPPI that PI ring of the MA is more planar with the benzene ring than that in the neutral DMAPPI (Table 1). Further, we have also calculated the minimum energy at different values of dihedral angle ϕ at an interval of 10° in the range of 0−180°. The potential energy curve (not shown) so obtained possesses an activation barrier of ∼37 kJ

(37) Mishra, A. K.; Dogra, S. K. *Spectrochim. Acta* **1983**, *39A*, 609.
(38) Krishnamurthy, M.; Phaniraj, P.; Dogra, S. K. *J. Chem. Soc., Perkin Trans. 2* **1986** 1917.
(39) Sinha H. K.; Dogra, S. K. *J. Photochem.* **1987**, *36*, 149.
(40) Jiang, Y. B. *J. Photochem. Photobiol.* **1994**, *78*, 205.
(41) Rettig, W. *Angew. Chem., Int. Ed. Engl.* **1986**, *25*, 971.

Table 2. Absorption Band Maxima (λ_{max}^{ab}, nm), Absorbance (*A*), Fluorescence Excitation Spectra Maxima (λ_{max}^{exc}, nm) Recorded at λ_{max}^{fl} in the Respective Solvent, and the Fluorescence Band Maxima (λ_{max}^{fl}, nm) of the Different Prototropic Species of DMAPPI Recorded in Different Solvents ([DMAPPI] = 0.5 × 10^{-5} M)

	λ_{max}^{ab} (A)		λ_{max}^{exc}		λ_{max}^{fl} (ϕ_{fl})	
species	methanol	water	methanol	water	methanol	water
MA		324		323		399(0.0033)
(H_- 14)						505(0.0083)
N	341	335			397(0.22)	415(0.011)
(pH 9)					475(0.067)	505(0.0026)
MCs[a]						
MC1		~335	312	310		
MC2					413(0.022)	416(0.003)
MC3	370	368	380	380	516(0.014)	525(0.0007)
DCs[b]						
DC1	292(0.075)	285(0.112)	294	284	345(0.087)	344(0.033)
DC2	330(0.013)	330(0.002)	330	330	403	424
DC3	409(0.18)	410(0.017)	404		494	493
TC (H_0 −10.4)		290		293		355(0.16)

[a] Methanol (0.001 M H_2SO_4) and water (pH 4). *b*Methanol (0.4 M H_2SO_4) and water (pH 0.98).

Table 3. Ground-State pK_a Value and Excited State pK_a Value (pK_a*) for Different Prototropic Equilibriums

equlibrium	pK_a	pK_a*
N−MA	10.9	11.0
MC−N	6.45	6.8
DC−MC	2.21	2.2
TC−DC	−3.0	

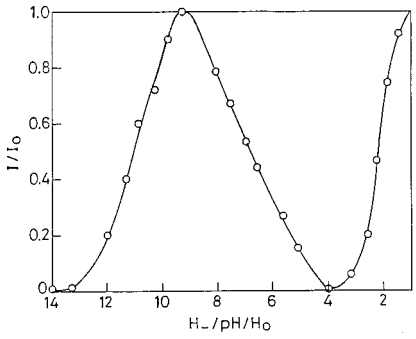

Figure 3. Plot of I/I_0 versus H_-/pH/H_0 for different prototropic equilibria.

mol^{-1}, which is very large as compared to thermal energy (RT). This suggests that the free rotation of PI ring around the C_2-C_{10} bond is not feasible at room temperature. Thus, a similar structure for TICT state of the MA of DMAPPI can be proposed, (i.e., the twisting of the $-NMe_2$ group and planarity of the PI ring) and is responsible for the enhancement of the TICT emission in the MA of DMAPPI. Kim et al.[42] in their study on DMABA have also shown that the hydrogen bonding at the electron-withdrawing group (carboxylic acid) plays the major role in increasing the TICT emission in aqueous cyclodextrins by making it more planar with benzene ring. To substantiate the above point, we have also carried out the AM1 calculations on DMABA and its MA. The results of AM1 calculations on the MA of DMABA establish that the $-COO^-$ group (−0.9°) is more coplanar with the benzene ring than the −COOH group (27°) in the neutral DMABA. Thus, the increase in TICT emissions observed in the MA of DMABA[40] and in our case over their neutral species could be more due to the increase in the coplanarity of the electron-withdrawing group with benzene ring.

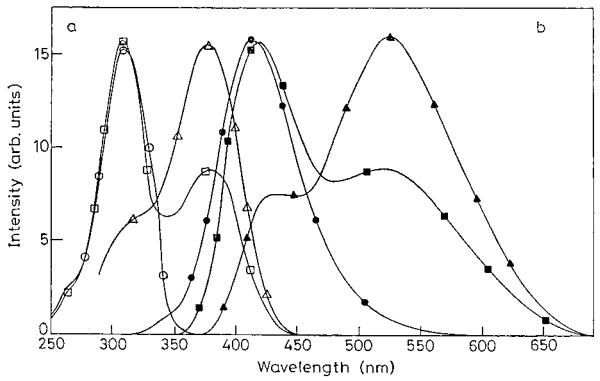

Figure 4. (a) Fluorescence excitation spectra of the MCs of DMAPPI in aqueous medium. pH 4.0, λ_{em} = 380 nm −○−; 500 nm −□−; 560 nm −△−. (b) Fluorescence spectra of the MCs of DMAPPI in aqueous medium. pH 4.0, λ_{exc} = 300 nm −●−; 350 nm −■−; 380 nm −▲−. [DMAPPI] = 0.5 × 10^{-5} M (for comparison all spectra are given in same scale).

4.2 Monocations. The absorption spectra of DMAPPI were recorded in methanol (10^{-3} M H_2SO_4) and water (pH 4). Figure 1 depicts the absorption spectra in aqueous media only, and data are compiled in Table 2. The absorption band maximum of the neutral DMAPPI is very large red shifted (368 nm), with a shoulder at ~335 nm, in comparison to the neutral species. The presence of an isosbestic point in the absorption spectra at 352 nm clearly suggests the equilibrium between the MC and the neutral or between the different MCs and the neutral DMAPPI. The pK_a value obtained for the (MC−N) prototropic equilibrium, using the Henderson equation, is found to be 6.45 (Table 3) with a slope of unity. The pK_a value for the prototropic equilibrium so obtained is greater than the similar prototropic equilibrium for any of the basic center (BI, BO, BT, pyridine, etc.) when present alone in the aromatic system.[43]

The fluorescence spectra of DMAPPI under the acidic conditions in both the solvents are much more complicated than the absorption spectra. For example, in water and at pH 4.0 (Figure 4b) only one fluorescence band is observed at 416 nm (ϕ_{fl} = 0.003) when $\lambda_{exc} \leq$ 340 nm. At $\lambda_{exc} \geq$ 350 nm another weaker band appears at 525 nm (ϕ_{fl} = 0.0007). The fluorescence intensity of the 525 nm increases and that of 416 nm band decreases with an

(42) Kim, Y. H.; Cho, D. W.; Yoon, M.; Kim, D. *J. Phys. Chem.* **1996**, *100*, 15670.

(43) Ireland, J. F.; Wyatt, P. A. H. *Adv. Phys. Org. Chem.* **1976**, *12*, 132.

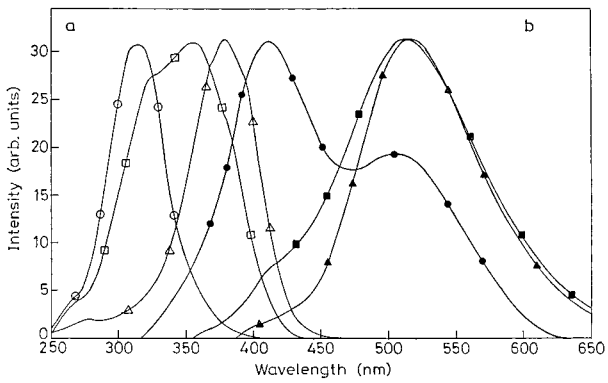

Figure 5. (a) Fluorescence excitation spectra of the MCs of DMAPPI in methanol. $[H_2SO_4] = 0.001$ M, $\lambda_{em} = 420$ nm −○−; 480 nm −□−; 540 nm −△−. (b) Fluorescence spectra of the MCs of DMAPPI in methanol. $[H_2SO_4] = 0.001$ M, $\lambda_{exc} = 300$ nm −●−; 350 nm −■−; 380 nm −▲−. $[DMAPPI] = 0.5 \times 10^{-5}$ M (for comparison all spectra are given in same scale).

increase of λ_{exc}. In methanol and at 0.001 M H_2SO_4 (Figure 5b), dual fluorescence is observed (413 nm, $\phi_{fl} = 0.022$; 516 nm $\phi_{fl} = 0.014$) when $\lambda_{exc} \leq 340$ nm and only one emission band (516 nm) is noticed when $\lambda_{exc} \geq 350$ nm. The red shifts observed in both the emission bands in water as a solvent when compared with those in methanol are larger for the LW (332 cm^{-1}) band than for the SW (175 cm^{-1}) band. Further, the ratio of $\phi_{fl}^{SW}/\phi_{fl}^{LW}$ increases from 1.57 to 4.29 in going from methanol to water as a solvent. The values of fluorescence band maxima and fluorescence quantum yields are independent of λ_{exc} in their appropriate regions.

The fluorescence excitation spectra of DMAPPI under acidic conditions and in both the solvents were recorded using λ_{em} in the range of 380−560 nm (Figures 4a and 5a). The behavior of the fluorescence excitation spectra in each solvent match with their corresponding emission in that solvent. In methanol (Figure 5a), only one band (380 nm) is observed in the excitation spectra when monitored in the range 480−560 nm and another band at 312 nm with a weak shoulder at 380 nm when monitored in the range of 380−460 nm. On the other hand, in water (Figure 4a) only one band at 310 nm is noticed in the excitation spectra when monitored in the range of 380−440 nm and band at 380 nm with shoulder at 310 nm (with decreasing intensity as the monitoring wavelength increases) when λ_{em} is in the range of 480−560 nm.

As mentioned previously, three kinds of MCs can be formed in DMAPPI. It is well established[43] that if $\pi \rightarrow p^*$ is the lowest energy transition the protonation at $-NMe_2$ group will lead to the blue shifts, whereas protonation at either of the $=N-$ atoms will lead to the red shifts in the absorption and fluorescence spectra of the neutral species. Fluorescence emission and excitation spectra suggest the presence of at least two kinds of MCs.

The data of Table 1 clearly indicate that under isolated conditions (gas phase or in nonpolar solvents) the MC2 is the most stable and the MC1 is the least stable. When dipolar solvation energy is also included in E_{iso}, the MC1 becomes the most stable and the MC2 the least. This is because the dipole moment of the MC1 in the ground state is very high (20.66 D) in comparison to other MCs. In other words, on the basis of these data, the MC1 should be the predominant ionic species in methanol or water as both these solvents have nearly similar $(\epsilon - 1)/(2\epsilon + 1)$ values. Similarly, the charge density data of the basic centers (at N_3 −0.1242, N_6 −0.1581, N_{16} −0.2656) also suggest that the first protonation should occur at the $-NMe_2$ group rather than at any other basic center ($=N_3-$, $=N_6-$). Observed experimental results that are different from those predicted above for the MCs can be explained as follows. The pK_a value for the protonation reaction of $-NMe_2$ in *N*,*N*-dimethylaminobenzene is 4.22,[44] whereas the pK_a values for the protonation of imidazole nitrogen ($=N_3-$) in 2-phenylbenzimidazole (PBI) is 5.23[37] and that of nitrogen ($=N_6-$) in pyridine is 5.2.[45] Our earlier results[22] have shown that the charge migration takes place from the $-NMe_2$ group to the $=N_3-$ atom and thus will decrease the pK_a value for the protonation of $-NMe_2$ group and increase the pK_a value for the protonation reaction of $=N_3-$ when compared with PBI. In other words, it is the relative increase or decrease in the charge density on the basic centers that plays the major role for their protonation, but sometimes the charge density data have led to the wrong assignments of the prototropic species.[46] Although the concept of an effective valance electron potential as a reactivity index for the protonation of azo heterocylic molecules in S_0 and S_1 is a good method,[47−49] we have calculated the global minima at the basic centers, using the potential energy mapping program.[50] This method also considers the charge densities at a particular basic center of interest plus the effective charges of rest of the atoms in the molecule. The greater the depth of the potential well, the greater will be the chances of protonation on the basic center. Figure 6 depicts the electrostatic potential energy map for DMAPPI using VSSPC program.[50] The results show that the site $=N_3-$ (MC2) is more reactive (−109.9 kJ mol^{-1}) than the site $=N_6-$ (−89.0 kJ mol^{-1}, MC3) and site $-NMe_2$ (−54.9 kJ mol^{-1}, MC1). This suggests that the chances of protonation are larger at $=N_3-$ and decrease in the order $=N_6-$ and $-NMe_2$ group. Thus, the results predicted by the potential energy mapping are similar to those observed by AM1 calculations without taking dipolar solvation into account but opposite when dipolar solvation energy is included in the AM1 calculations. The disagreement in the latter case could be due to the neglect of the solvation energy, which may increase the depth of the potential energy well around $-NMe_2$ group. In other words, both these models are unable to explain the site of protonation exactly when considered individually. Although it is not a good procedure, combining the results of both the models may give a qualitative picture about the proportion of these ions. On the basis of potential energy mapping, the preferable site of protonation is in the order of N_3 (MC2) > N_6 (MC3) > N_{16} (MC1) (−109.9, −89.0, −54.9 kJ mol^{-1} respectively), whereas based on the stability of the MCs in aqueous medium the order of stability is MC1 > MC2 > MC3. (0, +25.7, +84.8 respectively, Table 1). Combining the two results, though not feasible, gives the preferable site of

(44) Baddelay, G.; Chadwick, J.; Taylor, H. T. *J. Chem. Soc.* **1956**, 451.
(45) Liler, M. *Adv. Phys. Org. Chem.* **1975**, *11*, 267.
(46) Santra, S.; Dogra, S. K. *Chem. Phys.* **1996**, *207*, 103.
(47) Spanget-Larsen, J. *J. Chem. Soc., Perkin Trans. 2* **1985** 417.
(48) Waluk, J.; Rettig, W.; Spanget-Larsen, J. *J. Phys. Chem.* **1980**, *92*, 6930.
(49) Spanget-Larsen, J. *J. Phys. Org. Chem.* **1995**, *8*, 496 and references listed therein.
(50) Mishra, P. C.; Asthana, B. P. *Quantum Chemistry, QCEP Bull. Program No QCMP039* **1986**, *7*, 176.

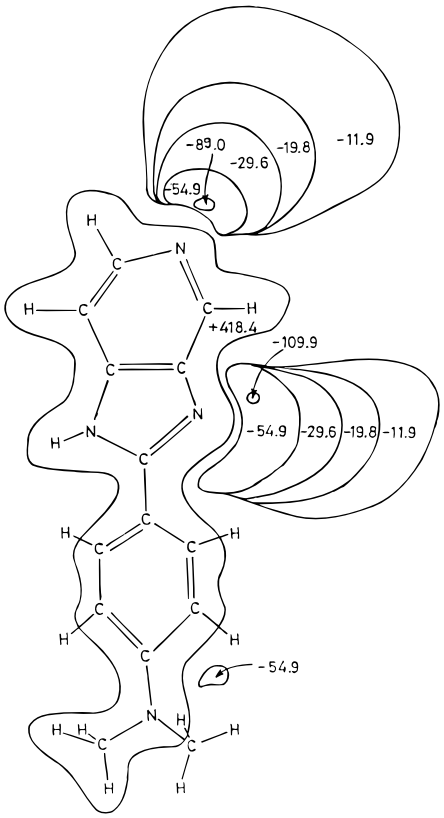

Figure 6. Electrostatic potential map for DMAPPI in the ground state (values shown are kJ mol^{-1}).

protonation in the order of MC3 > MC1 > MC2 (−63.3, −54.9, −25.1 kJ mol^{-1} respectively) and this order may be more favorable if the solvation energy is also included in the potential energy mapping. In other words the relative population of the respective species will be in the order of MC3 > MC1 > MC2 in the S_0 state. Thus, the absorption maximum at ∼370 nm can be assigned to the MC3 and the shoulder at ∼335 nm to the MC1 (see the following text also).

It has been established[38] that the spectral characteristics of the MC formed by protonating the imidazole nitrogen (═N_3−) in benzimidazoles are nearly similar to those of the neutral species if $\pi \rightarrow p^*$ is the lowest energy transition. Comparison of the 416 nm emission band of DMAPPI at pH 4 with that of the SW band of the neutral species in water suggests the formation of MC2. On the other hand, the corresponding fluorescence excitation spectrum (∼310 nm) does not match with the absorption spectrum (∼370 nm), which is large red shifted in comparison to that of the neutral species, but it is quite close to the ∼335 nm shoulder in the absorption spectrum and does match with the transition energy (306 nm) calculated for MC1 (Table 1). The difference observed in the excitation and absorption band of MC1 could be due to the overlap of the strong (∼370 nm) band with the weak 310 nm. The fluorescence excitation spectra recorded at emission wavelengths around 410 nm suggest that the ground-state species that gives rise to emission around 410 nm (i.e., the 416 nm emission) is MC1 (formed by the protonation of −NMe_2 group). This can be explained as follows. It is well-known[51] that −NH_3^+ or −$NHMe_2^+$ becomes a stronger acid and the ═N− atom becomes a stronger base on excitation to S_1 state. If the increase in the acidity and basicity of the respective group is very large in the S_1 state, the order of the protonation observed in the S_0 state may be reversed in the S_1 state and the phenomenon is known as biprotonic phototautomerism, observed in many molecules.[10−13,52−54] In other words, when MC1 (formed in the S_0 state) is excited to the S_1 state, −$NHMe_2^+$ dissociates to give −NMe_2 and the proton, which migrates to protonate the ═N_3− atom. This phenomenon is substantiated by: (i) the absence of ∼415 nm emission when excited at $\lambda_{exc} \geq 350$ nm in methanol. This is because the MC1 does not absorb at $\lambda > 350$ nm. (ii) The ϕ_{fl} of ∼415 nm in water is greater than that in methanol. This is because the −$NHMe_2^+$ ion will be a stronger acid in more polar medium (water) than in less polar solvent (methanol).[10−13,55] (iii) On the basis of the polarity of the MCs, the MC2 should be more stable than the other two MCs in nonpolar medium. We tried the cyclohexane/trifluoroacectic acid medium but were not successful because of the poor solubility of the molecule. However, in AOT/heptane reverse micelle[56] (dielectric constant ∼3 in the absence of water[57]), the fluorescence excitation spectra recorded at 400 nm give rise to a band maximum at 355 nm, which is different from 310 nm but resembles the results, which are consistent with when protonation occurs at the ═N− atom of the imidazole ring (═N_3−). So it indicates that the stability and thus the presence of the MC1 and MC2 in the S_0 state depends on the medium; i.e., MC1 will be present in the polar medium, whereas MC2 will be present in the nonpolar medium.

A very large red-shifted absorption band maximum at 370 ± 2 can be assigned to MC3. The data of Table 1 clearly indicate that the structural aspects of MC2 and MC3 are nearly similar in each aspect in the S_0 state (dihedral angles θ and ϕ; bond lengths C_2-C_{10} $C_{13}-N_{16}$); i.e., the ground-state geometry of each ionic species is planar. On the other hand, a large Stokes-shifted emission (∼8000 cm^{-1}) is observed at 525 nm, which is sensitive to the solvent polarity. Thus, suggesting that the LW emission of MC3 is possessing a charge-transfer character and based on the following arguments can be assigned to the TICT band. (i) By comparison of the Stokes shifts (∼6000 cm^{-1}) observed in the charge-transfer character of the MCs of the benzimidazoles (BIs),[38] the Stokes shift is large in the present case. (ii) The decrease in the ϕ_{fl} on protonation of the neutral BIs (10−30 times) is much larger than observed in case of DMAPPI (3.7 times). The large decrease in the ϕ_{fl} in the former cases could be due to the fact that the intramolecular charge tranfer (ICT) state is less stabilized and a $n \rightarrow p^*$ state is sufficiently low for favoring an alternative decay pathway such as intersystem crossing to the triplet state.[14] The presence of an additional basic center (═N_6−) in the latter molecule could enhance this intersystem crossing rate, and ICT emission is completely quenched in MC3. A similar behavior is also observed in case APPI.[25] The presence of the −NMe_2 group may enhance

(51) Shizuka, H. *Acc. Chem. Res.* **1985**, *18*, 141.
(52) Zalis, B.; Cepomacchia, A. C.; Jackson D.; Schulman, S. G. *Talenta* **1973**, *20*, 33.
(53) Kovi, P. J. Miller, C. L.; Schulman, S. G. *Anal. Chim. Acta* **1972**, *61*, 7.
(54) Kovi, P. J.; Schulman, S. G. *Anal. Chim. Acta* **1973**, *67*, 259.
(55) Sarpal, R. S.; Dogra, S. K. *J. Photochem.* **1987**, *38*, 263.
(56) Krishnamoorthy, G.; Dogra, S. K. Unpublished results.
(57) Bellete, M.; Lachapelle, M.; Durocher, G. *J. Phys. Chem.* **1990**, *94*, 5337.

the TICT emission. (iii) The Stokes shift observed in MC3 is similar to those observed in the molecules showing TICT behavior[41] and observed in case of the MA. (iv) Unfortunately, we could not carry out these experiments in nonpolar medium. However, in aqueous β-cyclodextrin,[56] no change is observed in the absorption spectra of MC3, but a large blue shift (492 nm) is observed in the fluorescence spectra similar to the TICT band of the neutral species. (v) The difference between the MC2 and the MC3 is that the MC2 can possess a resonance structure (MC2′, Scheme 2), which can increase the bond order in C_2-C_{10} and $C_{13}-N_{16}$. This will lead to more rigidity in the rings and the $-NMe_2$ group and the rotation around $C_{13}-N_{16}$ bond will be hindered. A similar kind of behavior is not possible in MC3. (vi) Unlike the absorption spectra (of MC3) or the fluorescence spectra of MC2, the fluorescence spectra of MC3 are red shifted compared to the fluorescence spectra of DC3 (see later), where similar to MC2, TICT emission is not possible because of the resonance structures DC3′ and DC3″ (Scheme 2). (vii) Last, the transition energy predicted for the LW band of MC3 also matches with the experimental results (Table 1).

The excited-state pK_a (pK_a*) value for the MC−N equilibrium, determined using fluorimetric titrations (Figure 3), is similar to the pK_a value. This suggests that the protonation or deprotonation rates are slower than the respective radiative rate constants. Relative fluorescence intensity (I/I_0) for the MCs could not be plotted because of their poor emission.

4.3 Dications. Absorption spectra of DMAPPI have been studied in methanol at 0.4 M H_2SO_4 and in water at pH 0.98. The relevant data are given in Table 2. Figure 1 depicts the absorption spectrum of the DCs in water only. Three band systems were observed in both the solvents, but the absorbance of each band system is different in each solvent. For example, in methanol, the absorbances at the band maxima 409, 330, and 292 nm are 0.18, 0.013, and 0.075, respectively, whereas those in water at 410, 330, and 285 nm are 0.017, 0.002, and 0.112, respectively. In comparison to the absorption band maximum of the MCs, the ∼410 nm band is largely red shifted, whereas the other two band systems are blue shifted. Similar to the MC−N equilibrium, only one pK_a value (2.2) is observed for the DC−MC equilibrium, having 308 and 422 nm as the isosbestic points.

The fluorescence spectrum of DMAPPI in methanol at 0.4 M H_2SO_4 and in water at pH 0.98 were studied by exciting at 290, 330, and 410 nm. The fluorescence spectra in methanol along with fluorescence excitation spectra are shown in Figure 7b,a, respectively. In all the cases only one fluorescence band is observed at each λ_{exc}. The fluorescence spectrum observed, when excited at 290 nm, is very large blue shifted (345 nm) and the structure can be described by the vibrational frequency of 1275 ± 50 cm^{-1} in both the solvents. The other two bands are broad and structureless, with emission maxima at ∼420 and 494 nm. The ratios of ϕ_{fl} DC1/DC2/DC3 are 1:0.097: 1.4×10^{-3} and 1:0.69:2.2×10^{-3} in methanol and water, respectively.

The fluorescence excitation spectra observed at each emission maximum give rise to the peaks, which resemble with the absorption band maxima (Figure 7a). The fluorescence excitation band observed at $\lambda_{em} = 520$ nm in water is very broad in comparison to that noticed in methanol, and thus, the error in locating the excitation band maximum is large.

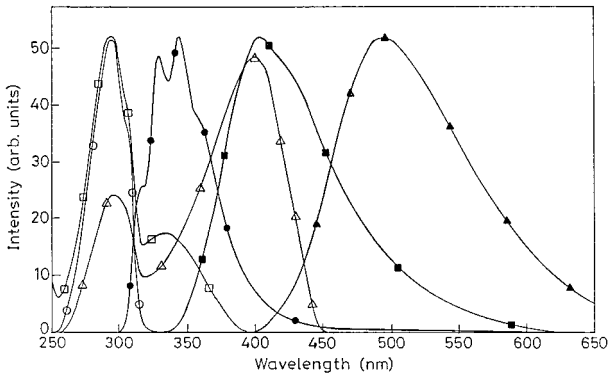

Figure 7. (a) Fluorescence excitation spectra of the DCs of DMAPPI in methanol. [H_2SO_4] = 0.4 M, λ_{em} = 345 nm −○−; 400 nm −□−; 500 nm −△−. (b) Fluorescence spectra of the DCs of DMAPPI in methanol. [H_2SO_4] = 0.4 M, λ_{exc} = 290 nm −●−; 330 nm −■−; 410 nm −▲−. [DMAPPI] = 0.5×10^{-5} M (for comparison all spectra are given in same scale).

Similar to the MCs, there can also be three possible dications (DC1, DC2, and DC3, Scheme 2) as mentioned earlier. Unlike the MCs, on the basis of the Maxwell−Boltzmann distributions and using the E_{sol} values of each DC (Table 1) the population ratio of DC1/DC2/DC3 is 1:3 $\times 10^{-6}$:8.3 $\times 10^{-3}$, respectively, in aqueous medium in the S_0 state. In other words, all three DCs will be present in both methanol and water in the S_0 state, but their populations will be different because of their ground-state dipole moments. The absorbance data (Table 2) of the three DCs are qualitatively in agreement with the population ratio. Quantitatively, it is not possible because of the absence of molecular extinction coefficients of the ionic species, which cannot be determined in our case. In the last section, we have established that MC1 and MC3 are the predominant monocations in the S_0 state, whereas MC2 and MC3 are the predominant monocations in the S_1 state. On the bais of the established results,[43] further protonation of either the $=N_3-$ or $=N_6-$ atom of the MC1 will lead to the red shifts in the absorption and fluorescence spectra of the MC1. The results of Table 2 show that one of the absorption (285 nm) and fluorescence (345 nm) band maxima of the DCs so formed at high acid concentrations are blue shifted with respect to the MC1 (λ_{max}^{exc} = 312 nm), as well as in comparison to the neutral species of DMAPPI, whereas the other absorption band (330 nm) is red shifted with respect to that of MC1 but slightly blue shifted in comparison to that of neutral DMAPPI. The first one is assigned to those of DC1 and the other to the DC2. This can be explained as follows: (i) As shown in Scheme 2, the positive charge in DC1 is only localized on the imidazole ring, whereas in case of DC2, the positive charge is delocalized over the complete PI ring. Due to this, the repulsion between the two positively charged rings will be more in the former than in the latter. This is shown by the dihedral ϕ, which is 49.4° in DC1 and 33.8° in DC2. Although this small difference in dihedral angle ϕ may not be enough to cause such a difference in the overlap of the π-cloud of the two rings and thus difference in the absorption maxima of DC1 and DC2, it will make some contribution to the difference between the absorption bands. (ii) It is also well-known that the protonation at the $=N-$ atom of the imidazole ring either in BI[38]

(neutral, 274 nm and the monocation, 274 nm) or in 2-PBI[37] (neural, 299 nm and the monocation 292 nm) does not lead to much change in the absorption spectrum of the neutral species of the respective moiety, whereas the protonation at the $=N-$ atom of the pyrido ring causes greater changes in the absorption spectrum. On protonation,[58] 6,8-bismethythiopurine (protonation on pyridine nitrogen) is red shifted by 24 nm, whereas 2,6-bismethylthiopurine (protonation on imidazole nitrogen, $=N_3-$) is red shited only by 5 nm. The second point may be playing the major role in the difference of absorption spectra of DC1 and DC2. A similar blue shift is also observed in the absorption spectrum of the MC1 of DMAPBI when the second protonation takes place (at the $=N-$ atom of the imidazole moiety).[22,23] The large Stokes shift (6020 cm^{-1}) observed in case of the DC1 suggests that the DC1 becomes more planar in the excited state. The vibrational structure present in the fluorescence spectrum substantiates this. The decrease in the ϕ_{fl} of the DC1 in going from methanol to water could be due to the solvent-induced fluorescence quenching. This is because (i) it is well-known that the $-NHMe_2^+$ ion[51] becomes a stronger acid in the S_1 state and its dissociation increases with the increase in the polarity of the medium. Further, the formation curve in the fluorimetric titration curve will give a different pK_a* value in comparison to pK_a. The results of Figure 3 give the same pK_a* (2.2) as nearly observed in the S_0 state (2.21). No change observed in the dissociation constant of DC1−MC1 equilibrium could be due to the smaller lifetimes of the conjugate acid−base pairs as compared to the inverse of the deprotonation and protonation rate constants of the respective acid and its conjugate base.

The absorption (330 nm) and fluorescence band maxima (424 nm) are assigned to the formation of the DC2. Besides the explanation given in the last paragraph, the relatively smaller population and the absorbance in comparison to other DCs explains the smaller fluorescence intensity of the ionic species DC2. The large Stokes shift (6720 cm^{-1}) in the DC2 can also be explained on similar lines as has been done for DC1. Last, the 410 nm absorption and 493 nm fluorescence maxima have been assigned to the DC3. The presence of three resonance structures (Scheme 2) suggests the presence of coplanarity between the two rings and is subtantiated by the dihedral angle ϕ (1.8°). The transition energy calculated for DC3 agrees nicely with the absorption maximum and in other DCs also the agreement is not bad (Table 1).

4.4 Trication. As shown, at H_0 −10.4, only one absorption band maximum (290 nm, Figure 1), one fluorescence maximum (355 nm) and similar fluorescence excitation spectra monitored at different emission wavelengths (Figure 8), confirm the presence of only one kind of trication (TC), obtained by protonating all the three basic centers, the $=N_3-$ and $=N_6-$ atoms, and the $-NMe_2$ group. The pK_a value determined from the absorption data is found to be −3. The excited-state pK_a value for the TC−DC equilibrium could not be determined because of the overlapping of the fluorescence intensities of the TC and DC.

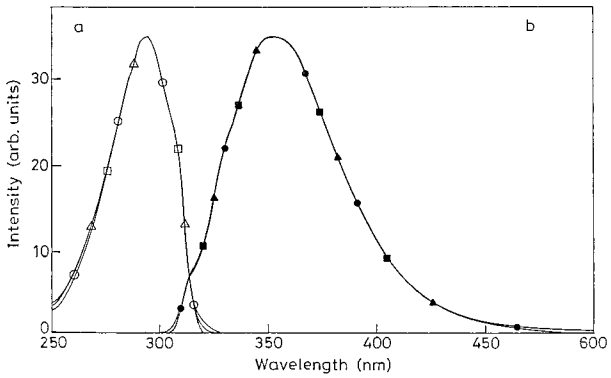

Figure 8. (a) Fluorescence excitation spectra of the TC of DMAPPI in aqueous medium. H_0 −10.4, λ_{em} = 300 nm −○−; 500 nm −□−; 560 nm −△−. (b) Fluorescence spectra of the TC of DMAPPI in aqueous medium. H_0 −10.4, λ_{exc} = 280 nm −●−; 290 nm −■−; 300 nm −▲−. [DMAPPI] = 0.5×10^{-5} M (for comparison all spectra are given in same scale).

5. Conclusions

On the bais of the absorption, fluorescence, and fluorescence excitation spectral characteristics and semiempirical quantum mechanical calculations, the following conclusions can be drawn. (i) Only one kind of MA is observed by deprotonating >N−H moiety. The SW emission is assigned to the normal band and LW emission to the TICT band. The increase in the TICT emission of the MA in comparison to the neutral one is due to the planar configuration of PI ring with benzene ring. (ii) MC1 and MC3 are present in the S_0 state and MC2 and MC3 in the S_1 state. Normal emission of MC3 is quenched due to the faster rates of nonradiative processes, and the TICT emission in MC3 can be explained on the same lines as for the MA. (iii) All three DCs are present, and their relative polulations depend on the nature of the solvents. (iv) Only one kind of TC is formed.

Acknowledgment. The authors are thankful to the Department of Science and Technology, New Delhi, for financial support under the project no. SP/S1/H-39/96.

JO9822986

(58) Reimann, U.; Bergmann, F.; Litchenberg, D.; Neiman, Z. *J. Chem. Soc., Perkin Trans. 1* **1973**, 793.